Available online at www.sciencedirect.com
SCIENCE DIRECT®
Journal of Power Sources 147 (2005) 241–248
JOURNAL OF POWER SOURCES
www.elsevier.com/locate/jpowsour

High-performance $LiCoO_2$ by molten salt ($LiNO_3$:LiCl) synthesis for Li-ion batteries

K.S. Tan, M.V. Reddy, G.V. Subba Rao, B.V.R. Chowdari *

Department of Physics, National University of Singapore, Singapore 117542, Singapore

Received 8 October 2004; accepted 15 January 2005
Available online 8 March 2005

Abstract

In an effort to increase and sustain the reversible capacity of $LiCoO_2$ on cycling, $LiCoO_2$ is prepared by using the molten-salt of the eutectic $LiNO_3$–LiCl at temperatures 650–850 °C with or without KOH as an oxidizing flux. The compounds are characterized by X-ray diffraction (XRD), scanning electron microscopy (SEM), chemical analysis, surface area and density techniques. Cathodic behaviour was examined by cyclic voltammetry (CV) and charge–discharge cycling. The 850 °C-synthesized $LiCoO_2$, which has excess lithium incorporated in to it, shows a reversible capacity, with ∼98% coulombic efficiency, of 167 (±2) mAh g^{-1} at a specific current of 30 mA g^{-1} in the range 2.5–4.4 V up to 80 cycles with no capacity-fading. When cycled to a higher cut-off voltage (4.5 V), a capacity of 192 (±2) mAh g^{-1} versus Li is obtained at the fifth cycle, but capacity-fading is observed, viz., ∼6% after 60 cycles. On the basis of the CV and capacity–voltage profiles, this is attributed to the non-suppression of the hexagonal (H1) ↔ (H1-3) structural transition. A similar capacity-fading, i.e., ∼5–6%, during 5–40 cycles, is also observed in the $LiCoO_2$ prepared at 650 and 750 °C when cycled up to only 4.3 V and this is ascribed to the non-suppression of the H1 ↔ M ↔ H1 phase transitions (M = monoclinic).

Keywords: $LiCoO_2$; Molten salt synthesis; Cathode material; Li-ion batteries; Capacity fading; Structural transition

1. Introduction

Lithium-transition metal oxides have been extensively studied for application as electrode materials for lithium–ion rechargeable batteries (LIB) [1]. At present layered $LiCoO_2$ is the preferred cathode (positive) material for LIBs due to its high volumetric energy density, excellent cycleability, and high operating cell voltage. $LiCoO_2$ is usually cycled to an upper cut-off voltage of 4.2 V versus Li and gives a specific capacity of ∼140 mAh g^{-1}. To obtain a higher capacity, $LiCoO_2$ must be charged to >4.2 V, but this will cause capacity fading on charge–discharge cycling. It is now known that the capacity-fading is due to crystal structure transitions taking place in $Li_{1-x}CoO_2$ as a function of x following Lithium de-intercalation (charge) and intercalation (discharge) [1,2]. These are reversible and occur at 4.06–4.18 V versus Li (hexagonal (H1) → monoclinic (M) → H1), at 4.55 V (H1 → hexagonal (H1-3)) and at 4.63 V((H1-3) → hexagonal (O1)). The H1 → M → H1 transitions are order–disorder type, whereas the H1 → (H1-3) involves drastic changes in the structure to form the so-called 'stage-II' $Li_{1-x}CoO_2$. The O1-phase formation from the (H1-3) phase involves a large change in the unit cell volume [2]. Hence, the volume changes of the unit cell that occur during these transitions cause 'electrochemical grinding' of the particles and result in a deterioration of the composite cathode and capacity fading. In addition, charging $LiCoO_2$ to >4.2 V will cause an increase in the electrode impedance as a result of the reaction of the charged cathode with the liquid electrolyte [2].

Studies have shown that the H1 → M → H1 transitions in $LiCoO_2$ can be easily suppressed by doping at the Co-site with ions such as Ni [3], Mg [4], Cr [5], Rh [6], Al [7,8],

* Corresponding author. Tel.: +65 6874 2956; fax: +65 6777 6126.
E-mail address: phychowd@nus.edu.sg (B.V.R. Chowdari).

0378-7753/$ – see front matter © 2005 Published by Elsevier B.V.
doi:10.1016/j.jpowsour.2005.01.019

or by incorporating excess Li to form $Li_{1+x}CoO_2$, $x \leq 0.15$ [3,4,9–12]. These doped compounds perform better when cycled up to 4.3 or 4.4 V, by way of smaller or no capacity fading in comparison with un-doped $LiCoO_2$. Studies have also shown that coating of the $LiCoO_2$ particles with oxides such as Al_2O_3, ZrO_2, SiO_2, $AlPO_4$ [2,13–19] helps to suppress capacity loss on cycling to >4.2 V, in some cases up to 4.5 V versus Li. The exact mechanism by which these electrochemically-inactive oxides act in a favourable manner is not clear at present [2].

The $LiCoO_2$ is usually prepared by high-temperature reaction in air or oxygen, using raw materials of oxides, carbonates, nitrates, or through chemical precursors via sol–gel, freeze-drying, etc. [1]. In all cases, heat treatment at >600 °C for extended periods is required to obtain the HT-$LiCoO_2$, which is electrochemically-active and possesses the rhombohedral–hexagonal α-$NaFeO_2$-type structure (the H1-phase). Molten-salt synthesis is a novel method to obtain highly crystalline pure and mixed oxides [20]. In favourable cases, nano-crystalline phases can also be prepared. The method has been recently used to prepare Mn-containing cathodes, $LiMn_2O_4$ [21,22] and $Li(Ni_{1/2}Mn_{3/2})O_4$ [23]. There are a few reports on the synthesis of $LiCoO_2$ using molten-salts and on studies of the cathodic properties. Han et al. [24] employed a LiCl–Li_2CO_3 eutectic mixture at 700–900 °C, but the compounds showed capacity fading when cycled in the range 2.8–4.2 V for 40 cycles. Phases $Li(Co_{0.8}M_{0.2})O_2$ in which M = Ni, Al were also prepared at 580 °C using a $LiNO_3$–LiOH eutectic, but their capacity was found to degrade within 20 cycles with an upper cut-off voltage of 4.3 V [25]. Liang et al. [26] also observed capacity-fading when cycled in the range 3.0–4.25 V in $LiCoO_2$ synthesized using KCl at 850 °C. When using KNO_3 as the molten-salt at 700 °C, however, Liang et al. [27] succeeded in preparing nano-particulate $LiCoO_2$ that gave excellent rate capability for up to 50 cycles when cycled the range 2.5–4.5 V.

This communication, reports the 'one-pot' synthesis of $LiCoO_2$ employing $LiNO_3$–LiCl eutectic as the molten-salt at 650–850 °C. The compound prepared at 850 °C shows a reversible capacity of 167 mAh g^{-1} with no capacity-fading when cycled in the range 2.5–4.4 V at 30 mA g^{-1} up to 80 cycles.

2. Experimental

$LiCoO_2$ was prepared at temperatures that ranged from 650 to 850 °C using LiCl (0.513 g, Merck) and $LiNO_3$ (6.068 g, Alfar Aesar) salts in the mole ratio 0.12:0.88 (eutectic composition) and $Co(NO_3)_2{\cdot}6H_2O$ (7.27 g, Merck). The mole ratio of Co: eutectic was kept at 1:4. After proper mixing, the mixture was placed in an alumina crucible and heated in air in a programmable box furnace (Carbolite, UK) to the desired temperature, at a heating rate of 3 °C min^{-1}. The heating was continued for 8 h at this temperature and the furnace was then shut off. After cooling to room temperature, the product was thoroughly washed with distilled water and decanted several times to remove excess lithium salts. The residue was dried in an air oven at 150 °C for 24 h and cooled. Free-flowing black powder was obtained. Synthesis was also carried out using added KOH to the molten salt eutectic in the mole ratio 0.2:1.0. In this case, the synthesis temperature was restricted to 650–750 °C, but the time of heating was 8 h. The compounds were recovered as described above.

Powder X-ray diffraction (XRD) patterns were obtained by means of a Siemens D5005 unit, Cu Kα radiation, to identify the crystal structure. The unit cell lattice parameters were obtained by the least-squares fitting method (2θ range, 10–70°) of the d-spacings and the hkl values. The morphology of powders was examined with a scanning electron microscope (SEM) (JEOL JSM-6700F). The Brunauer, Emmett and Teller (BET) surface area of the powder was measured with a Micromeritics Tristar 3000 (USA) instrument and density determination was undertaken with an AccuPyc 1330 pycnometer, Micromeritics (USA). The Li and Co contents were determined on selected compounds using an inductively coupled plasma (ICP) spectrometer (Thermo Jarrell Ash, IRIS/AP Duo).

Positive electrodes (cathodes) for the electrochemical measurements were fabricated from thoroughly ground active material, super P carbon black and a binder (Kynar 2801) in the weight ratio 70:15:15 using N-methyl pyrrolidone (NMP) as solvent. The doctor blade technique was employed. Etched Al-foil was the current-collector. Coin-type test cells were assembled in an Ar-gas filled glove box (MBraun, Germany), which maintained ≤1 ppm of H_2O and O_2 [28–30]. Lithium metal foil (Kyokuto metal Co., Japan) served as the negative electrode (anode) and 1 M $LiPF_6$ in ethylene carbonate (EC) + diethyl carbonate (DEC) (1:1, v/v) (Merck) as the electrolyte. Celgard 2502 membrane was used as the separator. Cyclic voltammetry and charge–discharge cycling at constant current were carried out at ambient temperature (RT) by a Mac-pile II system (Bio-logic, France) and a Bitrode multiple battery tester (Model SCN, Bitrode, USA). The cells were aged for 24 h before the cycling tests.

3. Results and discussion

3.1. Structure and morphology

As mentioned earlier, molten-salt synthesis is a novel one-pot method that give the oxides in quantitative yields. The salt can be recovered and re-used. The eutectic $LiNO_3$–LiCl (0.88:0.12 mol), which has a low melting point, 280 °C, is employed [28,31]. It is known that $LiNO_3$ and KOH are oxidizing fluxes, whereas LiCl is a non-oxidizing flux but acts as an excellent 'mineralizing' agent to give well-crystalline oxides [20–23]. During high-temperature treatment (650–850 °C), the added Co-nitrate decomposes to give the Co-oxide which dissolves in the flux and re-precipitates as $LiCoO_2$ after the formation of Co^{3+} ions and consumption of lithium from

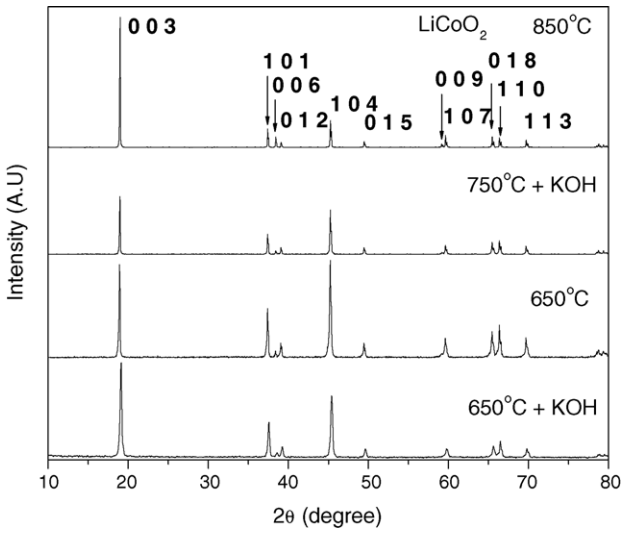

Fig. 1. X-ray diffraction patterns of $LiCoO_2$ synthesized using $LiNO_3$ + LiCl molten-salt at various temperatures. Miller indices (*h k l*) are shown.

$LiNO_3$. Due to the large content of salt, the consumption of $LiNO_3$ to form $LiCoO_2$ does not affect the composition of the eutectic. A similar mechanism operates when the LiCl–Li_2CO_3 eutectic is used for the preparation of $LiCoO_2$ [24]. Since KOH is also an oxidizing flux [20,32], its addition to the salt-eutectic in the present experiments, to the extent of 20 mole%, is presumed to help in the oxidation of Co^{2+} ions. K^+ ions do not get incorporated into the lattice of $LiCoO_2$ due to their smaller concentration in the molten salt and also because of the large difference in the ionic radius of Li^+ and K^+ ions [33].

The XRD patterns of $LiCoO_2$ prepared at various temperatures are presented in Fig. 1. All the peaks are indexed on the basis of the α-$NaFeO_2$ type, space group R $\bar{3}m$. No impurity lines are present. The hexagonal lattice parameters, *c*:*a* ratio and intensity ratio (*R*) of the (0 0 3) and (1 0 4) peaks are given in Table 1. The XRD patterns and the hexagonal *a* and *c* lattice parameters match well with those of $LiCoO_2$ reported in the literature that include those of the single crystals ($a = 2.8161(5)$ Å; $c = 14.0536(5)$ Å) [11,27,34–37]. The *c*:*a* ratio of 4.99 and the well-resolved splitting of the XRD lines assigned to the pairs of Miller indices (0 0 6, 1 0 2) and (1 0 8, 1 1 0) in all the compounds are good indication of a well-ordered hexagonal layered structure (Fig. 1 and Table 1). The *R* value of the 850 °C-prepared compound is 4.9, one of the largest values ever obtained, and this indicates that no 'cation-mixing' exists. It is noted, however, that the preferred orientation of the well-crystalline platelets may also be contributing to the large *R* value. With a decrease of the preparation temperature to 750 and 650 °C, the *R* value decreases to 1.3 and ∼1.0, respectively. A small amount of cation-mixing exists in the $LiCoO_2$ prepared at 650 °C due to exchange of small amounts of Li^+ and Co^{3+} ions from their octahedral sites in the respective layers. Addition of KOH to the flux during synthesis of $LiCoO_2$ at 650 °C improves the intensity ratio *R* from 1.0 to 1.5 (Fig. 1 and Table 1). In addition, the *c* lattice parameter shows a decreasing trend with increase in the synthesis temperature (Table 1). The *c* parameter of the 850 °C-synthesized $LiCoO_2$ is close to that of $Li_{1+x}CoO_2$, $x = 0.1$–0.2, as reported by Imanishi et al. [9], and suggests that there is excess Li incorporated into the lattice. Indeed, chemical analysis on duplicate samples of the compound showed $x = 0.15 \pm 0.01$. On the other hand, Levasseur et al. [3] reported only minor changes in the *a* and *c* lattice parameters in $Li_{1+x}CoO_2$, $x = 0$ and 0.1, prepared at 900 °C by a solid-state reaction. From chemical analysis of duplicate samples, the *x* value of $Li_{1+x}CoO_2$ prepared at 650 °C with KOH was found to be 0.03 ± 0.01 and this indicates that the compound has no excess Li^+ ions in the lattice.

Table 1
Hexagonal lattice parameters and *R* values of $LiCoO_2$ phases synthesized using molten salt ($LiNO_3$ + LiCl) at various temperatures

Synthesis temperature (°C)	*a* (±0.002 Å)	*c* (±0.005 Å)	*c*:*a*	I_{003}/I_{104} (*R*)
850	2.818	14.052	4.99	4.9
750 (+KOH)	2.818	14.056	4.99	1.3
650	2.818	14.072	4.99	1.0
650 (+KOH)	2.819	14.069	4.99	1.5

Detailed analysis of the data from application of a variety of physical, chemical and electrochemical techniques on $Li_{x0}CoO_2$, $x0 > 1.0$ led Levasseur et al. [12] to propose that the excess Li^+ ions occupy the Co sites in the Co layer and charge compensation is achieved by the creation of O vacancies. In addition, some of the Co^{3+} ions, adjacent to the O vacancies, occupy the square-based pyramidal sites instead of the octahedral sites and there by lead to an intermediate spin configuration, $Co^{3+(IS)}$. The general formula for $x0 > 1.0$ can thus be written as: $[Li]_{interslab}[Co^{III}_{1-3t}\ Co^{3+(IS)}_{2t}\ Li_t]_{slab}\ [O_{2-t}]$ where $t = (x0 - 1)/(x0 + 1)$ and Co^{III} represents Co^{3+} ion in the low-spin configuration, $t^6_{2g}e^0_g$. Accordingly, the electrochemical behaviour of $Li_{x0}CoO_2$ is expected to differ from that of $LiCoO_2$. Indeed, results from the literature [3,4,9–12] and present experiments show that $Li_{x0}CoO_2$ performs better as the cathode.

Scanning electron micrographs $LiCoO_2$ prepared at different temperatures are shown in Fig. 2. Agglomeration of well-crystalline, sub-micron particles of size between 0.5 and 1 μm with platelet morphology are present in $LiCoO_2$ prepared at 650 and 750 °C, Fig. 2(a) and (b). Similarly, $LiCoO_2$ prepared at 850 °C shows plate-like structures of 4–8 μm length and 1–2 μm thickness (Fig. 2(c)). Thus, the mineralization effect of LiCl in the molten slat is clearly revealed in all the preparations. The measured BET surface areas of the compounds are 1.07 and 1.96 $m^2\ g^{-1}$ (±0.03) for those synthesized at 650 with KOH and 850 °C, respectively. These values are typical of the oxide cathode materials prepared by the high-temperature reaction. The experimental density of $LiCoO_2$ powder prepared at 850 °C was 5.030 g cc^{-1} and compares well with the calculated X-ray density of 5.049 g cc^{-1}, which indicates that the particles are highly dense.

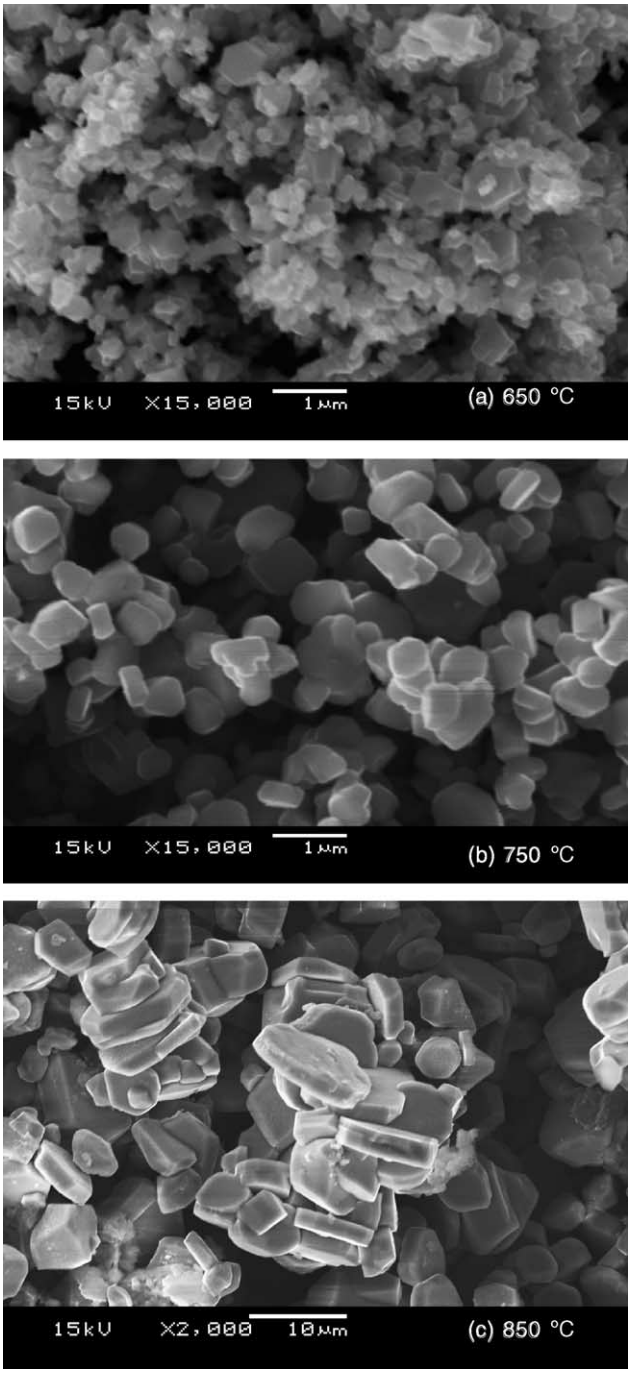

Fig. 2. Electron micrographs of as-prepared $LiCoO_2$ particles synthesized at: (a) 650 °C; (b) 750 °C; bar scale, 1 μm (c) 850 °C; bar scale, 10 μm.

3.2. Electrochemical studies

3.2.1. Cyclic voltammetry

Cyclic voltammetry is a well-suited and complementary technique to evaluate the cathodic performance and electrode kinetics of oxides [5,6,15,30,38,39]. It is also a sensitive technique in revealing the phase transitions that exist in $LiCoO_2$ during charge–discharge cycling [5,6,15,38]. The cyclic voltammograms (CV) of the cells were recorded with Li metal as the counter and the reference electrode, in the range 2.5–4.3, −4.4 and −4.7 V at ambient temperature, at a scan rate 0.058 mV s^{-1} up to 25 cycles. $LiCoO_2$ samples prepared at 650, 750 and 850 °C were used as the cathodes. Only selected cycles are shown in Fig. 3 for clarity. In the case of $LiCoO_2$ prepared at 650 °C with KOH, which has mole ratio of Li:Co = 1:1, the first-cycle anodic peak (de-intercalation of Li^+ ions from the host) occurs at ∼4.2 V (versus Li), whereas the main cathodic (intercalation of Li) peak is at ∼3.75 V. Minor (shoulder) cathodic peaks at 4.15, 4.04 V are also seen (Fig. 3a). In the second cycle, the anodic peak shifts to a lower voltage (∼4.10 V), but the corresponding cathodic peak shifts only slightly, by 0.20 V, to a higher voltage. The shift in the anodic peak voltage is an indication of the 'formation' of the electrode in the first-cycle, whereby the active material makes good electrical contact with the conducting carbon particles in the composite electrode, the current-collector and the liquid electrolyte. The shifts in the main anodic and cathodic peak voltages are complete by the fourth cycle and stabilize at 4.0 and 3.84 V, respectively. The hysteresis (ΔV = the difference between the sixth anodic and cathodic peak voltages) is 0.16 V, which demonstrates good reversibility of the charge–discharge reaction. Subsequent CV scans show that the ΔV, as well as the anodic and cathodic peak areas, remains almost constant with the cycle number, which again indicates good reversibility.

A similar behaviour of cyclic voltammograms was reported on the high temperature (HT)-synthesized O3-$LiCoO_2$ [15,38]. The major anodic/cathodic peaks just below 4.0 V were assigned to the $Co^{3+/4+}$ redox couple. In addition, the well-defined anodic peaks at 4.1 and 4.2 V and the corresponding cathodic peaks at 4.06 and 4.18 V that are observed from the 6th cycle onwards are due to reversible hexagonal (H1) ↔ monoclinic (M) ↔ H1 structural transitions of $LiCoO_2$ [2,5,15,34–36]. The voltammograms of $LiCoO_2$ prepared at 750 °C are similar to those prepared at 650 °C with KOH and are shown in Fig. 3(b). On the other hand, the ΔV value is slightly smaller and the structural phase transitions H1 ↔ M, M ↔ H1 are barely noticeable. The CV for $LiCoO_2$ up to 4.4 V prepared at 850 °C is presented in Fig. 3(c). As expected, the first two cycles are formation cycles similar to other CVs shown in Fig. 3(a) and (b). The hysteresis ΔV = 0.18 V and illustrates good reversibility. Interestingly, the H ↔ M ↔ H1 phase transitions are completely suppressed due to the excess lithium in $Li_{1.15}CoO_2$ [3,4,9–12]. Only the main anodic and cathodic peaks due to the $Co^{3+/4+}$ couple are present and the peak areas remain constant. It is also noted from Fig. 3(a)–(c) that between 2.5 and 3.3 V there is negligible electrochemical activity.

In order to reveal the H1 ↔ (H1-3) ↔ O1 phase transitions in $LiCoO_2$, CVs were recorded using a fresh cell in the range 2.5–4.7 V on the compound prepared at 850 °C. The first 12 cycles are shown in Fig. 3(d). For clarity, the CV for the third cycle is reproduced in Fig. 3(f). The 26th cycle CV of the $LiCoO_2$ prepared at 650 °C with KOH is given in Fig. 3(e). This is an extension of the CV of Fig. 3(a) recorded up to 25

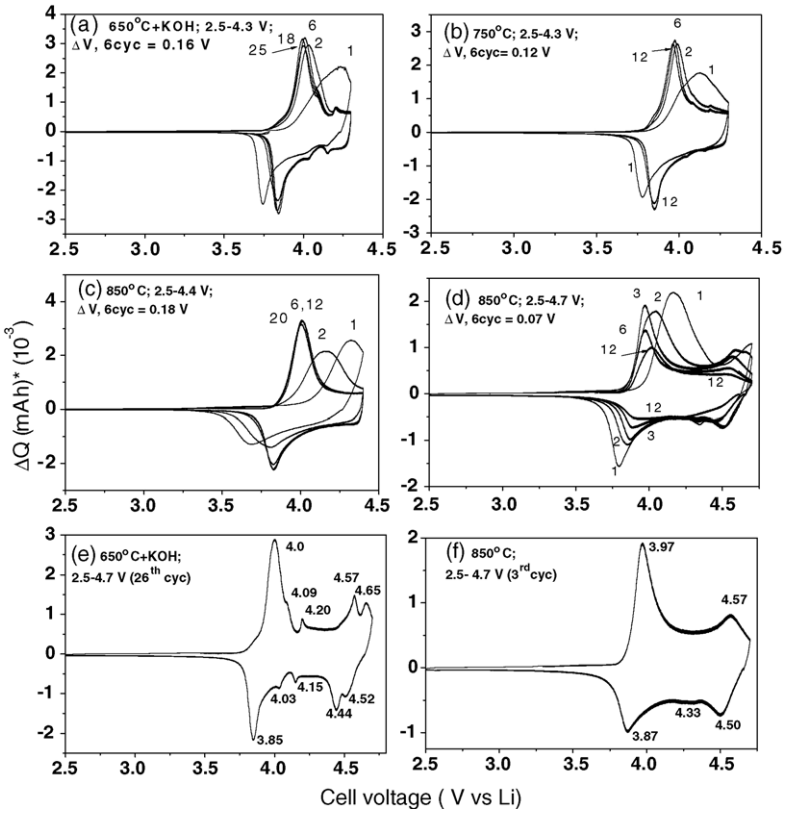

Fig. 3. Cyclic voltammograms of $LiCoO_2$ prepared at: (a), (e) 650 °C + KOH; (b) 750 °C; (c), (d), (f) 850 °C. Scan rate is 0.058 mV s^{-1}. Voltage ranges are shown. Numbers in (a)–(d) refer to cycle numbers. Numbers in (e)–(f) refer to voltages (±0.02 V).

cycles, in that the upper cut-off voltage has been increased to 4.7 V. As observed in Fig. 3(d) and (f), the 'formation cycle' is complete after two cycles. During 3–12 cycles, the main anodic and cathodic peaks for Li removal and insertion occur in the range 3.8–4.0 V, and the H1 ↔ M ↔ H1 transitions (range, 4.0–4.2 V) are completely suppressed. A broad unresolved anodic peak is present at 4.5–4.65 V during cycles 2–6. By contrast, there is a clear indication of the two phase transitions, O1 → (H1-3) at 4.50–4.55 V and (H1-3) → H1 at 4.37 V in the cathodic peaks (Fig. 3(d) and (f)). Due to the close proximity of the potentials, the anodic peak is not resolved into two well-defined peaks, but it is clear that, as has been observed in other studies [2], these transitions are reversible. With increase in the cycle number from 3 to 12 cycles, however, the areas under the main redox peaks due to the $Co^{3+/4+}$ couple decrease very significantly that is, continuous capacity fading is observed. This is due to the large unit-cell volume changes associated with the H1 ↔ (H1-3) ↔ O1 transitions and consequent electrochemical grinding of the particles of the active material and degradation of the composite electrode. Thus, cycling the 850 °C-synthesized $LiCoO_2$ to ≥4.5 V deteriorates the reversible capacity, whereas cycling to ≤4.4 V yields a stable and reversible capacity.

The peaks due to the $Co^{3+/4+}$ couple and the sequence of reversible phase transitions, H1 ↔ M ↔ H1 ↔ (H1-3) ↔ O1 are clearly illustrated in the 26th CV scan of $LiCoO_2$ prepared at 650 °C with KOH, as shown in Fig. 3(e). The anodic and cathodic peak voltages agree within ±0.02 V with those reported by Chen and Dahn [2] from differential-capacity curves. Thus, complimenting the chemical analysis data, the $LiCoO_2$ prepared at 650 and 750 °C, with or without KOH, do not have excess Li incorporated in the lattice. On the other hand, the excess Li in the compound prepared at 850 °C, $Li_{1.15}CoO_2$, enables the H1 ↔ M ↔ H1 transitions to be completely suppressed and the H1 ↔ (H1-3) ↔ O1 transitions are broadened or merged.

The CV scans were also recorded at various rates, from 0.058 to 0.464 mV s^{-1} for the 650 °C and the 850 °C synthesized $LiCoO_2$. With increase in the scan rate, the anodic peak voltage shifts to higher values, while that of the cathodic peak moves to lower voltage values. The respective ΔV values and the relative areas under the peaks also increase. The ΔQ, which is proportional to the peak current (i), is found to increase linearly against the square root of the scan rate and is an indication of transition from a finite to a semi-infinite diffusion process of the Li^+-ions within the crystal lattice of $LiCoO_2$ [38].

3.2.2. Galvanostatic cycling

Charge–discharge cycling of the cells with $LiCoO_2$ as cathodes were carried out up to 80 cycles at ambient temperature at a current density of 30 mA g^{-1}. For $LiCoO_2$ prepared at 850 °C, cycling was performed with upper cut-off voltages of 4.3, 4.4 and 4.5 V, whereas for compounds

Table 2
Observed charge and discharge capacities (±2 mAh g^{-1}), irreversible capacity loss (ICL) and capacity fading in $LiCoO_2$ prepared at various temperatures at current rate of (30 mA g^{-1})

Synthesis temperature; voltage range	Cycle 1		Cycle 5		Cycle 40		ICL (cycle 1)	Capacity fading (cycle range)
	Charge	Discharge	Charge	Discharge	Charge	Discharge		
850 °C; 2.5–4.3 V	161	147	157	157	157	157	14	Nil (5–40)
850 °C; 2.5–4.4 V	173	160	168	166	167	166	13	Nil (5–80)
850 °C; 2.5–4.5 V	208	187	194	191	187	186	21	6% (5–60)
750 °C + KOH; 2.5–4.3 V	171	161	160	158	–	–	10	5% (5–30)
650 °C; 2.5–4.3 V	184	166	167	164	156	155	18	6% (5–40)
650 °C + KOH; 2.5–4.3 V	178	156	158	156	149	148	22	5% (5–40)

synthesized at 650 and 750 °C, the voltage was only 4.3 V. In all cases, the lower cut-off voltage was 2.5 V. The representative voltage–capacity profiles of $LiCoO_2$ prepared at 850 °C (2.5–4.4 V) and at 650 °C with KOH (2.5–4.3 V) are shown in Fig. 4(a) and (b), respectively. For clarity, only select cycles are shown. The observed charge and discharge capacities are given in Table 2, and are plotted as a function of the cycle number in Fig. 5. During the first-charge process, there is a sudden increase in voltage to ∼3.8 V from the open-circuit voltage (∼3.0 V), followed by a plateau until about 35–50 mAh g^{-1} is reached, and then a gradual increase to the upper cut-off value. The plateau voltage is due to the co-existence of two phases with the compositions Li_xCoO_2, $0.94 \leq x \leq 0.75$, which are semiconducting ($x \geq 0.94$) and metallic ($x \leq 0.75$) [3,4,11,12].

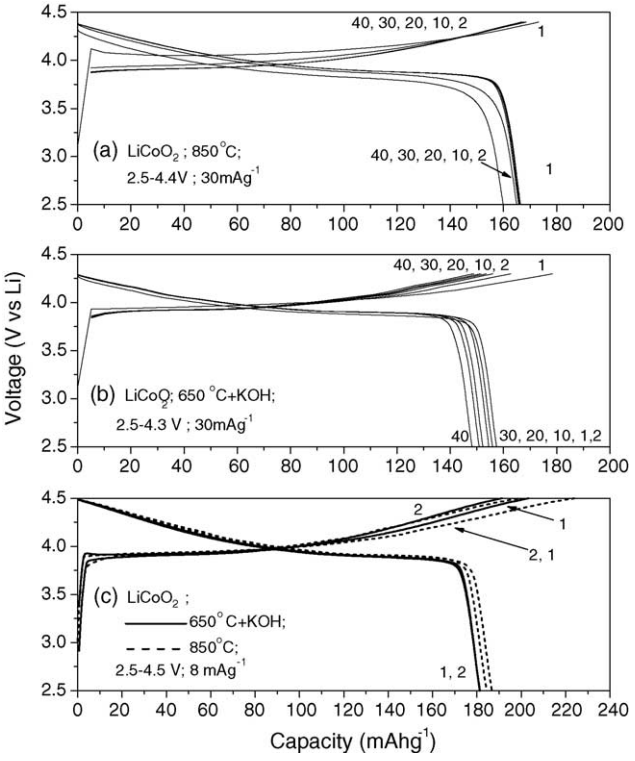

Fig. 4. Voltage vs. capacity profiles of $LiCoO_2$ prepared at: (a) 850 °C, 2.5–4.4 V; (b) 650 °C + KOH, 2.5–4.3 V, at current rate 30 mA g^{-1}; (c) 850 and 650 °C + KOH vs. Li-metal at current rate 8 mA g^{-1} for first two cycles. The numbers refer to cycle numbers. Voltage ranges are indicated.

In order to emphasize the plateau, charging was carried out at low current rate of 8 mA g^{-1} on fresh cells with $LiCoO_2$ prepared at 850 °C and at 650 °C with KOH in the range 2.5–4.5 V. These profiles, shown in Fig. 4(c), indicate the plateau clearly in the case of $LiCoO_2$ prepared at 650 °C with KOH, whereas the $LiCoO_2$ prepared at 850 °C, which has excess Li (viz., $Li_{1.15}CoO_2$), does not show the plateau. The latter behaviour is in accordance with that observed by Levasseur et al. [3,4,11,12] for $Li_{1.1}CoO_2$. The first-discharge and subsequent cycles do not show the plateaux implying a single-phase reaction in both cases.

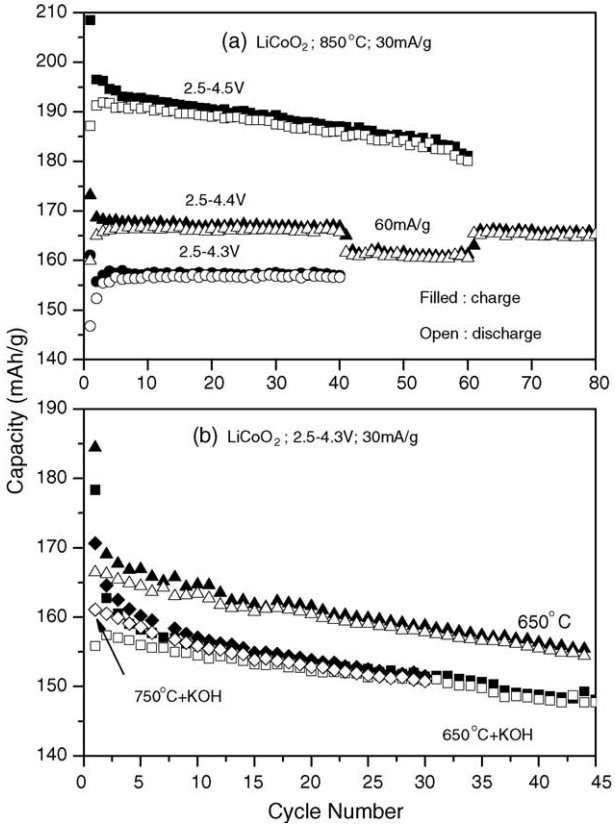

Fig. 5. Capacity vs. cycle number of $LiCoO_2$: (a) prepared at 850 °C in voltage ranges 2.5–4.3, −4.4, −4.5 V at current rate 30 mA g^{-1}; (b) prepared at 650 and 750 °C (with or without KOH) at current rate 30 mA g^{-1} in range 2.5–4.3 V at room temperature. Filled and open symbols represent charge–discharge capacity, respectively.

There is an irreversible capacity loss (ICL) between the first-charge and first-discharge capacity in all cases. For $LiCoO_2$ prepared at 850 °C, the ICL is only 13 ± 1 mAh g^{-1} with 4.3 and 4.4 V cut-off, whereas the value is 21 mAh g^{-1} with a 4.5 V cut-off. For $LiCoO_2$ prepared at 650 or 750 °C, the ICL varies in the range 10–22 mAh g^{-1} with a 4.3 V cut-off (Table 2). The 'formation cycle' of the cathode in the cell, however, extends to three to four cycles in all cases, after which consistent and reproducible charge and discharge capacities are observed. The capacity values at the fifth and 40th cycle, listed in Table 2 and shown in Fig. 5, indicate that the coulombic efficiency, represented by the difference between the charge and discharge capacity at a given cycle, is ~98% for all the $LiCoO_2$ phases. A reversible capacity of 157 (±2) mAh g^{-1} with no capacity fading during cycles 5–40 in the range 2.5–4.3 V at 30 mA g^{-1} is displayed by $LiCoO_2$ prepared at 850 °C. The same compound when cycled under the same conditions in a fresh cell, but in the range 2.5–4.4 V, shows a capacity of 167 (±2) mAh g^{-1} due to an increase of 0.1 V in the cut-off voltage. To test the rate capability, the current rate was increased to 60 mA g^{-1} at the end of 40 cycles. The capacity decreases to 163 mAh g^{-1} and remains stable for up to 60 cycles. When the current rate is switched back to 30 mA g^{-1}, the original capacity is recovered and remains stable for 80 cycles. It must be mentioned that the current density of 30 mA g^{-1} corresponds to ~0.2 C-rate assuming a reversible capacity of 167 mAh g^{-1}. The latter value corresponds to $x = 0.61$ in $Li_{1-x}CoO_2$. The observed excellent cycleability is due to the complete suppression of the H1 ↔ M ↔ H1 transitions that occur at $x = 0.5$ in $Li_{1-x}CoO_2$ (range, 4.0–4.2 V versus Li), as can be seen from the smooth charge–discharge profiles in Fig. 4(a) and is also clearly indicated in the CV scans (Fig. 3(c)).

The 850 °C-synthesized $LiCoO_2$, when cycled in a fresh cell to an upper cut-off voltage of 4.5 V at 30 mA g^{-1}, yields a discharge capacity of 191 (±2) mAh g^{-1} of the fifth cycle, which degrades to 180 (±2) mAh g^{-1} at the end of 60 cycles indicating ~6% capacity fading (Fig. 5(a), Table 2). The voltage–capacity profiles display an increase in the polarization of the electrode (not shown in Fig. 4(c), except for the first two cycles). It is noted that 191 mAh g^{-1} corresponds to $x = 0.7$ in $Li_{1-x}CoO_2$ and falls in the region of the H1 ↔ (H1-3) phase transition [2]. Since the CV in Fig. 3(d) and (f) clearly show that this transition is not suppressed in the 850 °C-prepared $LiCoO_2$, it obviously contributes to the observed capacity fading because of the large charges in unit cell volume during cycling. Similar capacity fading, by 5–6% during 5–40 cycles, is also shown by the 650 and 750 °C-synthesized (with or without added KOH) $LiCoO_2$, as can be seen in Figs. 4(b) and 5(b) and Table 2, even though the upper cut-off voltage is only 4.3 V. This is due to non-suppression of the H1 ↔ M ↔ H1 transitions, as is clear from the voltage plateau near 4.0–4.2 V in Fig. 4(b) and (c) (650 °C-preparation), and also clearly revealed in the CVs of Fig. 3(a),(b),(e) (650 and 750 °C-preparation). This behaviour is typical of undoped or uncoated polycrystalline $LiCoO_2$ prepared and processed by a variety of methods which are documented in the literature [2,40] and include molten salt synthesis [24–26].

4. Conclusions

Recent research is being focused on increasing and sustaining the reversible capacity on cycling of $LiCoO_2$ in order that this material can compete with the several suggested alternative oxide cathode materials for use in lithium-ion batteries. As a contribution to the effort, $LiCoO_2$ has been prepared using a molten salt of the eutectic $LiNO_3$–LiCl. The compounds were prepared at 650–850 °C with or without KOH added as an oxidizing flux. They were characterized by physical and electrochemical techniques. The 850 °C-synthesized $LiCoO_2$, into which an excess of lithium is incorporated, shows a reversible capacity, with ~98% coulombic efficiency, of 167 (±2) mAh g^{-1} at a current density of 30 mA g^{-1} in the range 2.5–4.4 V up to 80 charge–discharge cycles with no capacity fading. This is ascribed to the suppression of the H1 ↔ M ↔ H1 structural transitions, possibly due to the excess Li. Even though a higher capacity, viz., 192 (±2) mAh g^{-1} at the fifth cycle, is obtained when cycled to 4.5 V versus Li, capacity-fading is observed, i.e., ~ 6%, after 60 cycles. On the basis of CV and capacity–voltage profiles, this is attributed to the non-suppression of the H1 ↔ (H1-3) structural transition. A similar capacity fading, by ~5–6% during 5–40 cycles, is also observed with $LiCoO_2$ prepared at 650 and 750 °C (with or without added KOH) when cycled up to only 4.3 V. This behaviour is attributed to the non-suppression of the H1 ↔ M ↔ H1 transitions. In view of the simplicity and versatility of the molten-salt synthesis method, further improvement of the preparation of high-performance $LiCoO_2$ may be possible.

Acknowledgements

Thanks are due to M. Gupta, Mechanical Engineering Department, National University of Singapore, for help with scanning electron microscopy studies and to, Leng Lee Eng and Joanne Soong, Chemistry Department, National University of Singapore, for chemical analysis.

References

[1] W.A. Van Schalkwijk, B. Scrosati (Eds.), Advances in Lithium-Ion Batteries, Kluwar Acad./Plenum Publ, New York, USA, 2002.
[2] Z. Chen, J.R. Dahn, Electrochim. Acta 49 (2004) 1079.
[3] S. Levasseur, M. Ménétrier, C. Delmas, J. Electrochem. Soc. 149 (2002) A1533.
[4] S. Levasseur, M. Ménétrier, C. Delmas, J. Power Sources 112 (2002) 419.
[5] S. Madhavi, G.V. Subba Rao, B.V.R. Chowdari, S.F.Y. Li, Electrochim. Acta 48 (2002) 219.

[6] S. Madhavi, G.V. Subba Rao, B.V.R. Chowdari, S.F.Y. Li, J. Electrochem. Soc. 148 (2001) A1279.
[7] G. Ceder, Y.-M. Chiang, D.R. Sadoway, M.K. Aydinol, Y.-I. Jang, B. Huang, Nature 392 (1998) 694.
[8] S.T. Myung, N. Kumagai, S. Komaba, H.-T. Chung, Solid State Ionics 139 (2001) 47.
[9] N. Imanishi, M. Fujii, A. Hirano, Y. Takeda, M. Inaba, Z. Ogumi, Solid State Ionics 140 (2001) 45.
[10] N. Imanishi, M. Fujii, A. Hirano, Y. Takeda, J. Power Sources 97–98 (2001) 287.
[11] S. Levasseur, M. Ménétrier, E. Suard, C. Delmas, Solid State Ionics 128 (2000) 11.
[12] S. Levasseur, M. Ménétrier, S.-H. Yang, L. Gautier, A. Audemer, G. Demazeau, A. Largeteau, C. Delmas, Chem. Mater. 15 (2003) 348.
[13] Y.J. Kim, J. Cho, T.-J. Kim, B. Park, J. Electrochem. Soc. 150 (2003) A1723.
[14] Z. Chen, J.R. Dahn, Electrochem. Solid-State Lett. 6 (2003) A221.
[15] Y.J. Kim, H. Kim, B. Kim, D. Ahn, J.-G. Lee, T.-J. Kim, D. Son, J. Cho, Y.-W. Kim, B. Park, Chem. Mater. 15 (2003) 1505.
[16] H.-J. Kweon, J.J. Park, J.W. Seo, G.B. Kim, B.H. Jung, H.S. Lim, J. Power Sources 126 (2004) 156.
[17] J.-G. Lee, B. Kim, J. Cho, Y.-W. Kim, B. Park, J. Electrochem. Soc. 151 (2004) A801.
[18] H. Zhao, L. Gao, W. Qiu, X. Zhang, J. Power Sources 132 (2004) 195.
[19] S. Oh, J.K. Lee, D. Byun, W.I. Cho, B.W. Cho, J. Power Sources 132 (2004) 249.
[20] P. Afanasiev, C. Geantet, Coord. Chem. Rev. 178–180 (1998) 1725.
[21] X. Yang, W. Tang, H. Kanoh, K. Ooi, J. Mater. Chem. 9 (1999) 2683.
[22] W. Tang, X. Yang, Z. Liu, S. Kasaishi, K. Ooi, J. Mater. Chem. 12 (2002) 2991.
[23] J.-H. Kim, S.-T. Myung, Y.-K. Sun, Electrochim. Acta 49 (2004) 219.
[24] C.-H. Han, Y.-S. Hong, C.M. Park, K. Kim, J. Power Sources 92 (2001) 95.
[25] C.-H. Han, Y.-S. Hong, K. Kim, Solid State Ionics 159 (2003) 241.
[26] H. Liang, X. Qiu, S. Zhang, Z. He, W. Zhu, L. Chen, Electrochem. Commun. 6 (2004) 505.
[27] H. Liang, X. Qiu, H. Chen, Z. He, W. Zhu, L. Chen, Electrochem. Commun. 6 (2004) 789.
[28] K.M. Shaju, G.V. Subba Rao, B.V.R. Chowdari, Electrochem. Commun. 4 (2002) 633.
[29] N. Sharma, K.M. Shaju, G.V. Subba Rao, B.V.R. Chowdari, J. Power Sources 124 (2003) 204.
[30] K.S. Tan, M.V. Reddy, G.V. Subba Rao, B.V.R. Chowdari, J. Power Sources 141 (2005) 129.
[31] K.M. Shaju, K.V. Ramanujachary, S.E. Lofland, G.V. Subba Rao, B.V.R. Chowdari, J. Mater. Chem. 13 (2003) 2633.
[32] C. Shivakumara, M.S. Hegde, Proc. Indian Acad. Sci. (Chem. Sci.) 115 (2003) 447.
[33] R.D. Shannon, Acta Crystallogr. 32A (1976) 751.
[34] J.N. Reimers, J.R. Dahn, J. Electrochem. Soc. 139 (1992) 2091.
[35] T. Ohzuku, A. Ueda, J. Electrochem. Soc. 141 (1994) 2972.
[36] G.G. Amutucci, J.M. Tarascon, L.C. Klein, J. Electrochem. Soc. 143 (1996) 1114.
[37] J. Arimoto, Y. Gotoh, Y. Oosawa, J. Solid State Chem. 141 (1998) 298.
[38] S.-I. Pyun, H.-C. Shin, J. Power Sources 97–98 (2001) 277.
[39] K.A. Striebel, A. Rougier, C.R. Horne, R.P. Reade, E.J. Cairns, J. Electrochem. Soc. 146 (1999) 4339.
[40] Z. Chen, Z. Lu, J.R. Dahn, J. Electrochem. Soc. 149 (2002) A1604.